ELSEVIER

Biochimica et Biophysica Acta 1413 (1999) 139–146

BIOCHIMICA ET BIOPHYSICA ACTA
BBA

www.elsevier.com/locate/bba

Arylazido-β-alanine ADP-ribose, a novel irreversible competitive inhibitor of mitochondrial NADH-ubiquinone reductase

Marina V. Frenkin, Alexander B. Kotlyar *

Department of Biochemistry, George S. Wise Faculty of Life Sciences, Tel Aviv University, Ramat Aviv 69978, Israel

Received 11 June 1999; received in revised form 16 August 1999; accepted 21 September 1999

Abstract

Arylazido-β-alanine ADP-ribose, a photoreactive analogue of ADP-ribose, was synthesized. In the dark, arylazido-β-alanine ADP-ribose acts as a competitive reversible inhibitor of mitochondrial NADH-ubiquinone reductase with a K_i of 37 μM. Upon photolysis, arylazido-β-alanine ADP-ribose is converted to a potent irreversible active site-directed inhibitor of the enzyme. Photo-induced inhibition of membrane-bound NADH-ubiquinone reductase by arylazido-β-alanine ADP-ribose is incomplete and results in a 20-fold reduction of the NADH oxidase and 2.5-fold reduction of the energy-dependent NAD^+ reductase activities. The arylazido-β-alanine ADP-ribose resistant activities (direct and reverse) of the enzyme are characterized by a two orders of magnitude lower affinity to the corresponding substrates compared to those of the uninhibited NADH-ubiquinone reductase. A different kinetic behavior of the inhibited and native enzyme can be explained by invoking the two catalytically competent nucleotide-binding sites model of NADH-ubiquinone reductase.

Keywords: NADH-ubiquinone reductase; Arylazido-β-alanine ADP-ribose; Competitive inhibition; Bovine heart mitochondrion

1. Introduction

NADH-ubiquinone reductase (EC 1.6.5.3), commonly known as complex I, catalyzes electron transfer from NADH to ubiquinone and couples this process to proton translocation across the inner mitochondrial membrane. The isolated mitochondrial enzyme is composed of more than 40 individual subunits [1,2] and contains at least five iron-sulfur centers, a flavin mononucleotide moiety and tightly bound ubiquinone molecules, which participate in electron transfer from NADH to ubiquinone. Despite growing interest in the subject and an increased number of recent publications devoted to complex I, the catalytical mechanism of the enzyme is still far from being understood. Neither the sequence of intramolecular electron transfer reactions leading electrons from NADH to ubiquinone nor the number of the substrate-binding sites on the enzyme are known.

A wide variety of compounds are known to inhibit the NADH-ubiquinone reductase activity of the mitochondrial complex I. They are represented by a large number of non-competitive inhibitors, which act at or close to the ubiquinone reduction site [3–5], and a few competitive inhibitors that act at the nucleotide-binding site of the enzyme. The latter

Abbreviations: SMP, submitochondrial particle; arylazido-β-alanine, *N*-(4-azido-2-nitrophenyl) β-alanine; NADase, NAD^+ glycohydrolase

* Corresponding author. Fax: +972 (3) 6406834;
E-mail: s2shak@post.tau.ac.il

0005-2728/99/$ – see front matter
PII: S0005-2728(99)00091-2

class of inhibitors includes AMP, ADP, ATP [6] and NAD^+ [7,8], characterized by a low affinity to the enzyme, and ADP-ribose [9], as recently discovered by Vinogradov and coworkers, having a relatively high affinity to the active center of complex I.

Previous studies by Chen and Guillory [10] have shown that the arylazido-β-alanine analogue of NAD^+ acts as a competitive inhibitor of NADH-ubiquinone reductase in the dark. Light irradiation results in photo-dependent irreversible attachment of the analogue to the enzyme. The use of arylazido-β-alanine NAD^+ for studies of the catalytical mechanism of complex I was limited by insufficient affinity of the NAD^+ analogue to the enzyme. The insufficient affinity of the inhibitor leads to multi-site labelling of complex I and to a mixed type (competitive plus non-competitive) inhibition of its NADH-ubiquinone reductase activity [10].

The present communication describes the procedure for preparation of arylazido-β-alanine ADP-ribose, a strong competitive inhibitor of the mitochondrial NADH-ubiquinone oxidoreductase. The effect of arylazido-β-alanine ADP-ribose on NADH oxidase and on energy-dependent NAD^+ reductase activities of membrane-bound complex I has been investigated.

2. Materials and methods

All chemicals were obtained from Sigma Chemical Company.

2.1. Synthesis and purification of arylazido-β-alanine NAD^+

Arylazido-β-alanine NAD^+ was synthesized from arylazido-β-alanine and NAD^+ essentially as described by Chen and Guillory [10]. The mixture of products obtained after the synthesis, containing arylazido-β-alanine adducts and free NAD^+, was dissolved in 20 ml water. The pH of the solution was brought to 5.5 by addition of KOH. The solution was loaded onto a 100×10 mm DEAE-Sephadex column equilibrated with 5 mM Tris-HCl (pH 7.5). Arylazido-β-alanine NAD^+ and co-products of the synthesis were eluted from the column at 25°C with 5 mM Tris-HCl (pH 7.5) at a flow rate of 0.5 ml/min by a linear KCl gradient from 0 to 1 M over a period of 2 h. Arylazido-β-alanine NAD^+ elutes from the column at 0.15 M KCl. Chromatography on a DEAE column enabled complete purification of arylazido-β-alanine NAD^+ from arylazido-β-alanine containing co-products of the synthesis and free arylazido-β-alanine. The latter compounds were eluted from the column in KCl concentrations higher than 0.2 M. Arylazido-β-alanine NAD^+ fractions eluted from the DEAE column contained free NAD^+. Further chromatography of the compound on a C-4 reversed-phase high performance liquid chromatography column, 250×4.6 mm (Vydac, Hesperia, CA, USA), enabled separation of the labelled dinucleotide from the unlabelled one. The unlabelled dinucleotide was eluted from the column in 5 mM CH_3COONa (pH 5.5) at a flow rate of 0.8 ml/min, while arylazido-β-alanine NAD^+ was eluted from the column in 50% methanol. Methanol was removed from arylazido-β-alanine NAD^+ by chromatography of the latter on DEAE-Sephacell. Arylazido-β-alanine NAD^+, eluted from C-4 column, was diluted five times with water and loaded onto a 100×10 mm DEAE-Sephacell column equilibrated with 5 mM CH_3COONa (pH 5.5). The labelled dinucleotide was eluted from the column in 200 mM KCl. The relative absorbance ratio of the purified arylazido-β-alanine NAD^+ at 260 and 475 nm is equal to 8.3.

2.2. Photolysis

Submitochondrial particles (SMPs) were diluted with 50 mM Tris-Cl (pH 8.0), mixed with arylazido-β-alanine ADP-ribose and irradiated by a TM-36 transilluminator (UVP, San Gabriel, CA, USA) in a glass microcuvette. The short UV light generated by the transilluminator was completely filtered by the glass wall of the cuvette and the sample was irradiated mostly by 320–350 nm light. Irradiation of SMPs in the absence of arylazido-β-alanine ADP-ribose did not result in complex I inactivation.

2.3. Enzyme assay

SMPs were prepared and coupled with oligomycin as described [11]. The protein content was determined with Biuret reagent. NADH oxidase and NAD^+ reductase activities were measured at 25°C

in 1 ml of assay solution containing 0.25 M sucrose, 0.1 mM EDTA, 20 mM Tris-Cl (pH 8.0) and 1 mg/ml bovine serum albumin (BSA). NADH oxidase reaction was initiated by addition of 7 μg SMP to the assay solution supplemented with 100 μM NADH. NADH-ferricyanide reductase reaction was initiated by addition of 7 μg SMP to the assay solution supplemented with 1 mM ferricyanide, 100 μM NADH and 1 mM KCN. NADH-ubiquinone reductase was initiated by addition of 3 μg SMP to the assay mixture supplemented with 20 μM 2,3-dimethoxy-5-methyl-6-decylbenzoquinone, 100 μM NADH, 1 mM KCN and 0.4 μg/ml gramicidin. The succinate-supported NAD^+ reductase reaction was initiated by simultaneous addition of 2 mM NAD^+ and 20 mM succinate-K to the assay solution containing 14 μg/ml SMP. NADPH oxidase reaction was measured at 25°C in a 0.4 ml microcuvette (0.2 cm optical path). The reaction was initiated by addition of 10 μg SMP to 0.4 ml of the assay solution containing 0.25 M sucrose, 100 mM Na-P_i (pH 6.0), 1 mg/ml BSA, 0.5 mM NADPH and 0.4 μg/ml gramicidin. SMPs were pretreated with butanedione as described [12] in order to suppress transhydrogenase activity. The initial rates of NAD(P)H oxidation or NAD^+ reduction were followed at 340 nm ($\varepsilon_{mM} = 6.2$).

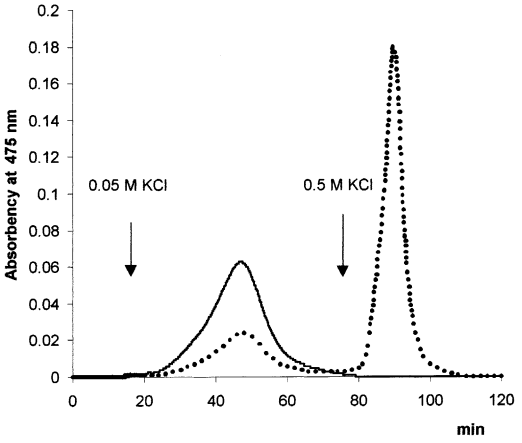

Fig. 1. Chromatography of NADase-treated arylazido-β-alanine NAD^+ on DEAE-Sephacel. Arylazido-β-alanine NAD^+ (1.3 mM) was treated with NADase (0.02 U/ml) at 37°C in 20 mM HEPES (pH 7.0). One ml of 1.3 mM arylazido-β-alanine NAD^+ solution before (solid line) and after 30 min hydrolysis with NADase (dotted line) was loaded onto a 100×10 mm DEAE-Sephacell column equilibrated with 5 mM CH_3COONa (pH 5.5) and was eluted by KCl. The arrows indicate addition of 0.05 and 0.5 M KCl to the column buffer.

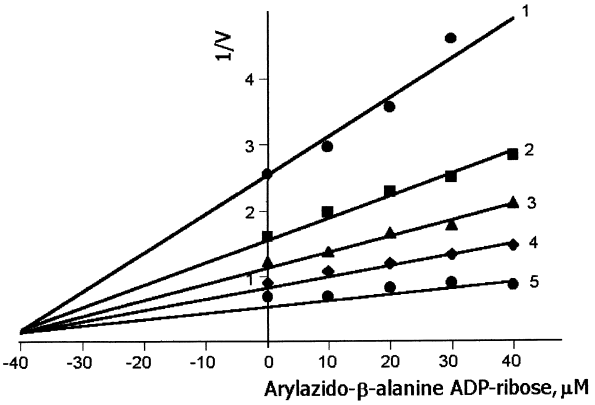

Fig. 2. Competitive inhibition of the NADH oxidase by arylazido-β-alanine ADP-ribose. The initial rate of NADH oxidation (V) was measured as described in Section 2 in the presence of 0.5 (curve 1), 1 (curve 2), 1.5 (curve 3), 2.5 (curve 4) and 3.5 μM NADH (curve 5). The dependences of initial rates of the reaction on the concentration of arylazido-β-alanine ADP-ribose are presented in Dixon coordinates. V is expressed in μmol NADH oxidized per min per mg protein.

3. Results

3.1. Preparation of arylazido-β-alanine ADP-ribose

We have used chromatographically purified arylazido-β-alanine NAD^+ as a starting material for preparation of arylazido-β-alanine ADP-ribose. Arylazido-β-alanine NAD^+ prepared as described in Section 2 is characterized by absorption maxima at 475 and 260 nm. The relative absorbance ratio at 260 and 475 nm of arylazido-β-alanine NAD^+ obtained in this work is equal to 8.3. This value is higher than the value of 7.6 reported earlier by Chen and Guillory [10]. The probable reason for the difference in the absorbance ratios for arylazido-β-alanine NAD^+ obtained in this and in the earlier studies is a higher purification level of the compound achieved in the present work by column chromatography.

Chromatographically purified arylazido-β-alanine NAD^+ was subjected to enzymatic hydrolysis with NAD^+ glycohydrolase (NADase) (EC 3.2.2.5). Enzymatic hydrolysis of arylazido-β-alanine NAD^+ results in two products: nicotinamide and arylazido-β-alanine ADP-ribose. The positively charged nico-

tinamide elutes from a DEAE column in void volume. Arylazido-β-alanine ADP-ribose, carrying a charge of −2, elutes from the column at higher salt concentrations than the non-hydrolyzed arylazido-β-alanine NAD^+, carrying a charge of −1 (see Fig. 1). Arylazido-β-alanine ADP-ribose obtained by the above procedure has characteristic absorption maxima at 475 and 260 nm. The ratio of absorbances of the compound at 260 and 475 nm is equal to 7.5, a value which is less than the value (8.3) estimated in this work for arylazido-β-alanine NAD^+. The difference in the relative absorbances of both compounds at 260 nm corresponds to the contribution of the nicotinamide group to the net absorbance of arylazido-β-alanine NAD^+ at this wavelength.

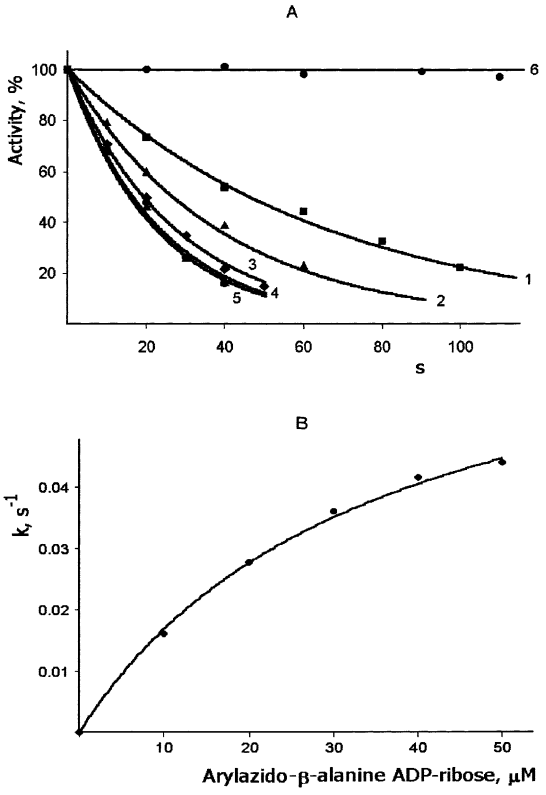

Fig. 3. Light-induced irreversible inhibition of complex I by arylazido-β-alanine ADP-ribose. A: SMPs (0.5 mg/ml) were placed in a 1 mm path glass microcuvette and irradiated (see Section 2) for the time indicated on the figure in the presence of 10 (curve 1), 20 (curve 2), 30 (curve 3), 40 (curve 4), 50 (curve 5) and 50 μM arylazido-β-alanine ADP-ribose plus 10 mM ADP-ribose (curve 6). The power of the excitation light was 8-fold reduced by a neutral density filter. NADH-ferricyanide reductase activity of the irradiated particles was measured as described in Section 2. One hundred percent activity corresponds to 9.5 μmol NADH oxidized per min per mg protein. The continuous curves are single exponential best-fit approximations of the experimental data. B: The dependence of the rate constant (k) of photo-inactivation on the arylazido-β-alanine ADP-ribose concentration. The rate constants were estimated from single exponential analysis on A. The solid curve is a best-fit hyperbolic approximation of the dependence of the rate constant on the inhibitor concentration. The values of k_{max} and K_i (the inhibitor concentration at which k is equal to half of k_{max}) are correspondingly equal to 0.076 s^{-1} and 35 μM and were obtained from the hyperbolic fitting.

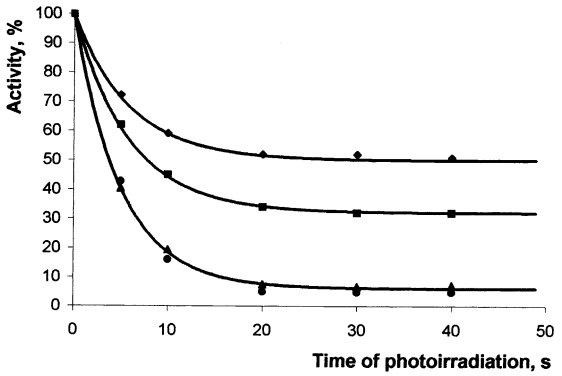

Fig. 4. Inhibition of NADH-ferricyanide, NADH oxidase, NADPH oxidase and energy-dependent NAD^+ reductase activities by arylazido-β-alanine ADP-ribose. SMPs (30 μg/ml) were activated (see [11]) with 1 μM NADH for 2 min at 25°C and irradiated by 320–350 nm light in the presence of 20 μM arylazido-β-alanine ADP-ribose for a time indicated on the figure (see Section 2). NADH-ferricyanide reductase (▲), NADH oxidase (●), NADPH oxidase (◆) and succinate-supported NAD^+ reductase reactions (■) were assayed as described in Section 2. One hundred percent activities correspond to 9.5 and 1.16 μmol NADH oxidized, 0.11 μmol NADPH oxidized and 0.25 μmol NAD^+ reduced per min per mg protein for NADH-ferricyanide reductase, NADH oxidase, NADPH oxidase and NAD^+ reductase reactions, respectively. Irradiation of the particles for 2 min in the presence of 10 mM ADP-ribose did not result in reduction of either of the above-mentioned enzymatic activities.

3.2. *Inhibition of NADH-ubiquinone reductase by arylazido-β-alanine ADP-ribose*

Fig. 2 depicts a kinetic analysis of reversible inhibition of NADH oxidase activity of SMPs in the dark by arylazido-β-alanine ADP-ribose in Dixon plots. As evident from the figure, arylazido-β-alanine ADP-ribose acts as a competitive inhibitor of the enzyme with a K_i value of 37 ± 5 μM. The affinity of arylazido-β-alanine ADP-ribose to the enzyme is much higher than that of arylazido-β-alanine NAD^+. The latter had no effect on the rate of NADH oxi-

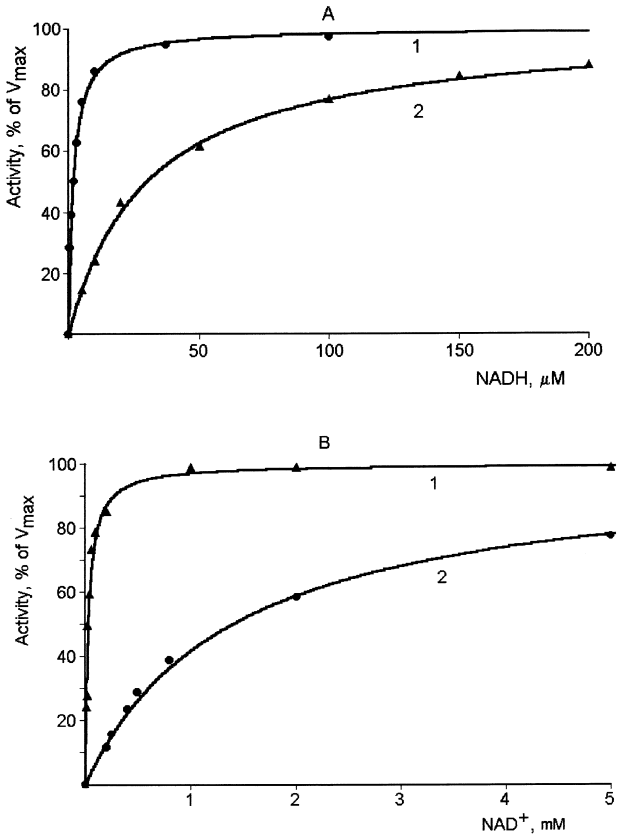

Fig. 5. Kinetics of NADH-ubiquinone reductase and succinate-supported NAD^+ reductase reactions catalyzed by native and arylazido-β-alanine ADP-ribose-treated SMPs. SMPs were pretreated with 2 μM NADH for 2 min at 25°C and irradiated for 1 min in the presence of 20 μM arylazido-β-alanine ADP-ribose as shown in Fig. 4. NADH-ubiquinone reductase (A) and NAD^+ reductase (B) reactions of native (curves 1) and photo-inactivated SMPs (curve 2) were assayed at different substrate concentrations as described in Section 2. Dependences of the initial rates of NADH-ubiquinone reductase and NAD^+ reductase reactions on the dinucleotide concentration are depicted on the figure. Solid curves correspond to single hyperbolic fits with the following parameters: $K_m = 1.0$ μM, $V_{max} = 1.17$ μmol/min mg; $K_m = 30$ μM, $V_{max} = 0.16$ μmol/min mg; $K_m = 37$ μM, $V_{max} = 0.29$ μmol/min mg; $K_m = 1.8$ mM, $V_{max} = 0.13$ μmol/min mg for curves 1 and 2 of A and curves 1 and 2 of B, respectively.

dation at concentrations lower than 50 μM (data not presented). A higher affinity of arylazido-β-alanine ADP-ribose compared to that of arylazido-β-alanine NAD^+ corresponds nicely with the recent data of Vinogradov and coworkers [9], demonstrating a high affinity of the ADP-ribose molecule to the active site of complex I.

Irradiation of SMPs by 320–350 nm light in the presence of arylazido-β-alanine ADP-ribose causes time-dependent irreversible inhibition of NADH-ferricyanide activity of complex I (see Fig. 3A). The photo-dependent inhibition is completely prevented by ADP-ribose, a competitive inhibitor of the enzyme [9]. Protection of the enzyme from photo-inactivation by ADP-ribose supports the competitive nature of the arylazido-β-alanine ADP-ribose-induced inhibition. The activity of the enzyme decreases exponentially with the time of irradiation in the presence of arylazido-β-alanine ADP-ribose. In order to slow the photo-inactivation process down, the excitation power was reduced eight times with a neutral density filter. The pseudo-first order rate constant of inactivation estimated by single exponential fitting of the data on Fig. 3A depends hyperbolically on the concentration of arylazido-β-alanine ADP-ribose (see Fig. 3B). The hyperbolic dependence of the inactivation rate on the inhibitor concentration indicates that the mechanism of irreversible inhibition of complex I includes formation of specific reversible complex between the enzyme's active center and arylazido-β-alanine ADP-ribose and further light-induced attachment of the inhibitor to the protein. The dissociation constant of 35 ± 5 μM was estimated for the enzyme arylazido-β-alanine ADP-ribose complex by hyperbolic analysis of the dependence of the inhibition rate on the concentration of arylazido-β-alanine ADP-ribose (see Fig. 3B). This value is equal within the experimental error to the value of K_i for reversible inhibition of NADH oxidase activity by the analogue (see Fig. 2).

Irreversible inhibition of NADH-ferricyanide reductase, NADH oxidase, NADPH oxidase and succinate-supported NAD^+ reductase activities of the enzyme by arylazido-β-alanine ADP-ribose is shown in Fig. 4. As seen in the figure, a final level of light-induced inhibition, established during irradiation of SMPs in the presence of 20 μM arylazido-β-alanine ADP-ribose, is different for NADH oxidase, NADPH oxidase and NAD^+ reductase activities. The rates of NADH-ferricyanide reductase and NADH oxidase reactions are reduced by 93–95%, NAD^+ reductase activity by 65% and NADPH oxidase activity by 50%. Partial inhibition of the reactions is not the result of an insufficient concentration of the inhibitor. A three-fold increase of the arylazido-β-alanine ADP-ribose concentration did not re-

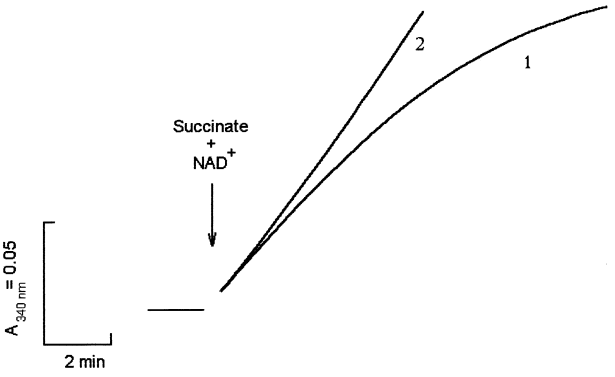

Fig. 6. Time-course of the succinate-supported NAD^+ reduction catalyzed by native and arylazido-β-alanine ADP-ribose-inhibited SMPs. Curve 1, SMPs (20 μg/ml) were pre-incubated with 2 μM NADH in a glass microcuvette filled with 1 ml of the assay solution (see Section 2) for 2 min at 25°C in order to obtain maximum NAD^+ reductase activity. Curve 2, SMPs (60 μg/ml) were pre-activated with NADH as described above and irradiated by 320–350 nm light in the presence of 10 μM arylazido-β-alanine ADP-ribose for 1 min as described in Section 2. The reaction was initiated by simultaneous addition of NAD^+ (2 mM) and succinate-K (20 mM) to the assay solution.

sult in a stronger inhibition of either of the enzymatic activities (data not shown). Inactivation of any of the above-mentioned activities is completely prevented by ADP-ribose, which is indicative of the competitive nature of the inhibition.

The residual fraction of the enzyme, left uninhibited after treatment with arylazido-β-alanine ADP-ribose, is characterized by a low affinity to NADH and NAD^+. K_m for NADH estimated for the untreated enzyme is equal to 1.0 μM, while the value estimated for the arylazido-β-alanine ADP-ribose-treated enzyme is equal to 30 μM (see Fig. 5A). The affinity of NAD^+ to the inhibited and the native enzyme is significantly different as well. K_m values for NAD^+ in NAD^+ reductase reaction catalyzed by arylazido-β-alanine ADP-ribose-treated and the native enzyme (see Fig. 5B) are 1.8 mM and 37 μM, respectively. Kinetic parameters for the arylazido-β-alanine ADP-ribose-treated and the uninhibited enzyme are summarized in Table 1. As evident from Table 1, the arylazido-β-alanine ADP-ribose-inhibited enzyme catalyzes NAD^+ reductase and NADH oxidase reactions with similar maximum rates. The native enzyme is more efficient in catalyzing the direct reaction.

Fig. 6 demonstrates the time-course of NAD^+ reduction driven by oxidation of succinate as catalyzed by uninhibited and arylazido-β-alanine ADP-ribose-treated SMPs. After oxidation of a small amount of NADH (the event required for activation of complex I [11]), succinate and NAD^+ were added simultaneously. The rate of NADH accumulation progressively slows down as a result of enzymatic oxidation of generated NADH. A high affinity of uninhibited complex I to NADH and a high rate of NADH oxidation compared to the NAD^+ reduction result in strong suppression of the reverse reaction even at low concentrations of accumulated NADH (curve 1 of Fig. 6). The inhibited enzyme characterized by low affinity to NADH and a low rate of NADH oxidation (see Table 1) displays almost a linear dependence of product formation in time (curve 2 of Fig. 6).

4. Discussion

In the present study, we have shown that arylazido-β-alanine ADP-ribose has a high affinity to the active center of complex I. In the dark, it acts as a competitive reversible inhibitor of the enzyme with

Table 1
Catalytic properties of native and arylazido-β-alanine ADP-ribose-inactivated SMPs

Reaction	SMPs		Inactivated SMPs[a]	
	K_m^b, μM	V_{max}^b, μmol/min/mg	K_m^b, μM	V_{max}^b, μmol/min/mg
NADH-ubiquinone reductase	1.0	1.17	30	0.16
NAD^+ reductase	37	0.29	1 800	0.13

[a]SMPs were irradiated by 320–350 nm light in the presence of 20 μM arylazido-β-alanine ADP-ribose for 1 min as shown in Fig. 4.
[b]Estimated as shown in Fig. 5.

K_i value of 37 μM (see Fig. 2). When photo-irradiated, arylazido-β-alanine ADP-ribose causes irreversible inhibition of the enzyme. Complete protection of the enzyme from irreversible inactivation by ADP-ribose (see Fig. 3A) and a hyperbolic dependence of the inactivation rate on the concentration of arylazido-β-alanine ADP-ribose (see Fig. 3B) indicate that inactivation of the enzyme proceeds through formation of a specific complex between the enzyme's active center and the inhibitor. The affinity binding constant of 35 μM was estimated for arylazido-β-alanine ADP-ribose by analysis of the dependence of the rate of irreversible inhibition on the concentration of the inhibitor (see Fig. 3B). The latter value corresponds nicely with the value of K_i estimated for the reversible inhibition of the enzyme by arylazido-β-alanine ADP-ribose.

The high affinity of ADP-ribose [9] and its arylazido-β-alanine analogue (present work) to the active center of complex I compared to that of NAD^+ [7,8] may be explained by assuming the presence of positively charged amino acid residue(s) close to the location of the nicotinamide group of the dinucleotide in the active center of complex I. The electrostatic repulsion between the proposed positively charged amino acid residue and the oxidized nicotinamide group may account for a rather low affinity of NAD^+ to the active center of the enzyme. Elimination of the nicotinamide's positive charge either by NAD^+ reduction or by removing the nicotinamide group results in a considerable increase of affinity of the molecule to the enzyme. The two orders of magnitude higher affinity of NADH [8] and ADP-ribose [9] to the active center of complex I compared to that of NAD^+ [7,8] supports the above suggestion.

Photo-irradiation of SMPs in the presence of arylazido-β-alanine ADP-ribose results in incomplete inhibition of the enzyme. The rates of NADH-ferricyanide reductase and NADH-ubiquinone reductase reactions are reduced by 93–95%, while NAD^+ reductase activity dropped only by 65%. The affinity of the arylazido-β-alanine ADP-ribose resistant NADH oxidase and NAD^+ reductase activities of the enzyme to their corresponding substrates are lower by two orders of magnitude as compared to those of the uninhibited NADH-ubiquinone reductase (see Table 1).

Different sensitivities of the reverse and direct reactions catalyzed by complex I to arylazido-β-alanine ADP-ribose inhibition are consistent with the proposal of two catalytically competent nucleotide-binding sites on the enzyme. The arylazido-β-alanine ADP-ribose sensitive site, having a high affinity to the dinucleotide, is more specific with respect to NADH oxidation. On the other hand, the arylazido-β-alanine ADP-ribose insensitive site, having a low affinity to NAD^+ and NADH, catalyzes the reverse and the direct reactions with almost equal maximum rates (see Table 1). The difference in sensitivities of the forward and backward reactions of complex I to arylazido-β-alanine ADP-ribose is consistent with the observation of Zharova and Vinogradov [9] on the unidirectional nature of ADP-ribose-induced inhibition of the enzyme. A strong competitive inhibition of NADH oxidation by ADP-ribose and inability of ADP-ribose to suppress energy-dependent NAD^+ reductase reaction led the authors to stipulate the existence of two unidirectional nucleotide-binding sites on complex I, one catalyzing the direct and another the reverse reaction. According to our data, each of the suggested active sites is capable of catalyzing both the reverse and the direct reactions. The relative efficiencies of these sites in driving NADH oxidation and NAD^+ reduction are, however, significantly different.

Fifty percent reduction of NADPH oxidase activity by arylazido-β-alanine ADP-ribose demonstrated in this work is also consistent with the two catalytically competent nucleotide-binding sites on complex I, contributing equally to the overall rate of NADPH oxidation.

A large number of subunits comprising complex I leaves room for speculations on the location of the arylazido-β-alanine ADP-ribose sensitive and insensitive sites on the enzyme molecule. Two nucleotide-binding motifs located on the 51 kDa [13] and on the 39 kDa [1] subunit of complex I may be possible candidates. A high affinity of arylazido-β-alanine ADP-ribose enables to selectively label the active site of complex I and to determine the subunit to which the inhibitor is attached. These experiments are underway at present in our laboratory and include covalent attachment of arylazido-β-alanine ADP-ribose to the active center of isolated complex I and subsequent identification of the labelled subunit.

References

[1] I.M. Fearnley, J.E. Walker, Conservation of sequences of subunits of mitochondrial complex I and their relationships with other proteins, Biochim. Biophys. Acta 1140 (1992) 105–134.
[2] J.E. Walker, J.M. Skehel, S.K. Buchanan, Structural analysis of NADH: ubiquinone oxidoreductase from bovine heart mitochondria, Methods Enzymol. 260 (1995) 14–34.
[3] M.D. Esposti, Inhibitors of NADH-ubiquinone reductase: an overview, Biochim. Biophys. Acta 1364 (1998) 222–235.
[4] H. Miyoshi, Structure-activity relationships of some complex I inhibitors, Biochim. Biophys. Acta 1364 (1998) 236–244.
[5] P. Lümmen, Complex I inhibitors as insecticides and acaricides, Biochim. Biophys. Acta 1364 (1998) 287–296.
[6] Y. Hatefi, K.E. Stempel, W.G. Hanstein, Inhibitors and activators of the mitochondrial reduced diphosphopyridine nucleotide dehydrogenase, J. Biol. Chem. 244 (1969) 2358–2365.
[7] Y. Hatefi, K.E. Stempel, Isolation and enzymatic properties of the mitochondrial reduced diphosphopyridine nucleotide dehydrogenase, J. Biol. Chem. 244 (1969) 2350–2357.
[8] A.D. Vinogradov, Kinetics, control, and mechanism of ubiquinone reduction by the mammalian respiratory chain-linked NADH-ubiquinone reductase, J. Bioenerg. Biomembr. 25 (1993) 367–375.
[9] T.V. Zharova, A.D. Vinogradov, A competitive inhibition of the mitochondrial NADH-ubiquinone oxidoreductase (Complex I) by ADP-ribose, Biochim. Biophys. Acta 1320 (1997) 256–264.
[10] S. Chen, B.J. Guillory, Arylazido-β-alanine NAD^+ an NAD^+photoaffinity analogue, J. Biol. Chem. 252 (1977) 8990–9001.
[11] A.B. Kotlyar, A.D. Vinogradov, Slow active/inactive transition of the mitochondrial NADH-ubiquinone reductase, Biochim. Biophys. Acta 1019 (1990) 151–158.
[12] L. Djavadi-Ohaniance, Y. Hatefi, Oxidation of NADPH by submitochondrial particles from beef heart in complete absence of transhydrogenase activity from NADPH to NAD, J. Biol. Chem. 250 (1975) 9397–9403.
[13] S.J. Pilkington, J.M. Skehel, R.B. Gennis, J.E. Walker, Relationship between mitochondrial NADH-ubiquinone reductase and a bacterial NAD-reducing hydrogenase, Biochemistry 30 (1991) 2166–2175.